

Frequency Estimation in DSOGI cells by means of the Teager Energy Operator

Alberto Pigazo, Francisco J. Azcondo, Christian Brañas
Universidad de Cantabria
 Santander, España
 [pigazoa, azcondof, christian.branas}@unican.es

Paula Lamo
Universidad Internacional de La Rioja
 Logroño, España
 paula.lamo@unir.net

Abstract— Second Order Generalized Integrator (SOGI) cells are used for notch filtering due to their simplicity and their harmonic rejection capability. SOGI and Dual SOGI (DSOGI) filter cells, combined with Frequency Locked Loops (FLL) to adjust the notch frequency, are commonly used in both 1 ϕ and 3 ϕ grid following (GFL) power converters for synchronization, i.e. SOGI-FLL and DSOGI-FLL, respectively. The FLL relies on a gradient descent method to minimize a cost function built up around one inner SOGI cell variable, e.g., the in-quadrature voltage estimation, and one outer variable, i.e. the error signal due to the SOGI filter cell. As a result, the FLL manages relatively large DC offsets and harmonic distortion passing through the outer SOGI cell variable, which deteriorates the frequency estimation and then, the SOGI-FLL performance. To attenuate such issues, the method proposed in this digest only uses inner SOGI cell variables. It minimizes the deviation between the estimated grid frequency and the frequency of the signal across the SOGI cell, which is detected through the Teager Energy Operator (TEO). The proposal is validated in simulation and experimentally.

Index Terms—PLL, synchronization, three-phase, converter, second order generalized integrator.

I. INTRODUCTION

Second Order Generalized Integrator (SOGI) and Dual SOGI (DSOGI) filter cells, included in the structure of Frequency Locked Loops (FLL), are usually employed in 1 ϕ and 3 ϕ grid following (GFL) power converters for synchronization due to their simplicity and harmonic rejection capability. Firstly proposed in [1], [2], the SOGI-FLL circuit (Fig. 1) has become an standard and multiple variants have been proposed and analyzed in technical literature [3], [4], including the effect on the GFL stability [5], [6]. As shown in [7], [8], the FLL in [1] consists in a frequency estimator based on the gradient descent method: the objective function, J , to be minimized by adjusting the estimated grid frequency, ω' , is build up from one inner SOGI cell variable, e.g. the in-quadrature voltage, qv'_α , and one outer SOGI cell variable, i.e. the SOGI filter error, e , resulting in

$$J = \frac{e^2}{2} = \frac{(v_g - v'_\alpha)^2}{2} \quad (1)$$

$$\dot{\omega}' = -\gamma_{FLL} \frac{\partial J}{\partial \omega'}, \quad (2)$$

where γ_{FLL} adjusts the speed of the gradient descent. Different objective functions are evaluated in [7] and [9] but the FLL principle in [1] remained unchanged, i.e. combining inner and outer SOGI cell variables, which is due to overall SOGI-FLL cell simplicity and performance, e.g. fast adaptation to grid frequency variations. Normalization can be included as a

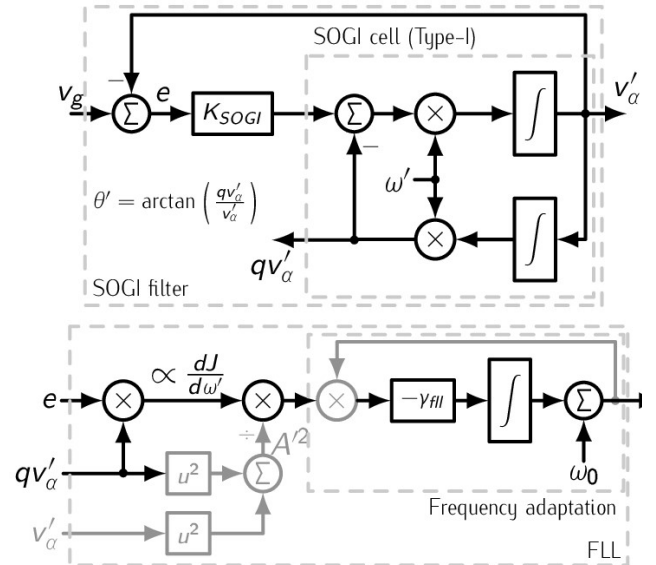


Fig. 1. Type I SOGI-FLL.

feedforward action [5], as shown in gray color in Fig. 1. However, relatively large DC offsets and harmonic distortion levels exist in outer SOGI cell variables, which must be managed by the gradient descent method, whose filtering capabilities are limited due to the use of one integrator.

A novel approach is proposed here to estimate the grid frequency where only inner SOGI cell variables are used. To this extent, the Teager Energy Operator (TEO) [10] is used to evaluate the frequency of the signal across the SOGI cell and adjust the estimated grid frequency accordingly. The resulting SOGI-TEO cell is described in Section 2. It is used for synchronization in a 3 ϕ -3 ω GFL converter and compared with the DSOGI cell both in simulation, in Section 3, and experimentally, in Section 4. Finally, conclusions are given.

II. PROPOSED SOGI-TEO CELL

Under ideal operation conditions and steady state, $v_g(t) = A \cos(\omega t)$ and the type I SOGI cell in Fig. 1 results in

$$\begin{cases} v'_\alpha(t) = A \cos(\omega t) \\ qv'_\alpha(t) = A \sin(\omega t) \end{cases} \quad (3)$$

Moreover, the SOGI filter results in $e = 0$, and the FLL provides $\omega' = \omega$.

Then, by applying the continuous form of the TEO [10], given by

This work has been supported by the Ministry of Science and Innovation through the project RTI2018-095138-B-C31: "Electrónica de potencia aplicada a la red eléctrica y a procesos industriales": PEGIA.

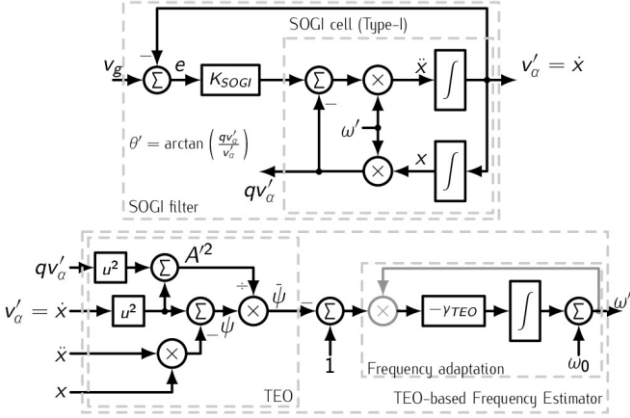


Fig. 2. Proposed SOGI-TEO cell.

$$\psi(x(t)) = \dot{x}^2(t) - x(t) \ddot{x}(t), \quad (4)$$

to v'_α in (3), results in

$$\psi(v'_\alpha(t)) = \psi(qv'_\alpha(t)) = A^2 \omega^2, \quad (5)$$

providing an estimation of the energy associated to v_g and, hence, its amplitude and frequency. However, with (5), no direct comparison of ω and ω' is achieved, and similarly occurs if $x(t) = qv'_\alpha$ and (4) are used.

A further inspection of (4) reveals that, to obtain an energy estimation, the signal processed must be almost a pure sinusoidal and two derivatives, or, alternatively, two integrators are needed. The Type-I SOGI cell in Fig. 1 accomplish both requisites. Then, the SOGI cell provides the required derivatives by selecting

$$x(t) = \frac{qv'_\alpha(t)}{\omega'(t)} = \frac{A}{\omega'(t)} \sin(\omega t), \quad (6)$$

and, then, having slow enough updates of $\omega'(t)$, under the assumptions above,

$$\begin{cases} \dot{x}(t) \approx A \frac{\omega}{\omega'(t)} \cos(\omega t) = v'_\alpha(t) \\ \ddot{x}(t) = -A \frac{\omega^2}{\omega'(t)} \sin(\omega t). \end{cases} \quad (7)$$

From (6) and (7), and evaluating (4), deviations of the estimated grid frequency related to the SOGI cell frequency are obtained, by

$$\frac{\psi\left(\frac{qv'_\alpha(t)}{\omega'(t)}\right)}{A^2} = \frac{\omega^2}{\omega'^2} = \bar{\psi}. \quad (8)$$

If the frequency estimation, ω' , matches the frequency of the signal across the SOGI cell, ω , then, from (8), $\bar{\psi} = 1$. Values above or below one implies that the estimated grid frequency is below or above the SOGI cell frequency, respectively. This can be used, as shown in Fig. 2, to build the SOGI-TEO cell, where only inner SOGI cell variables are used for frequency estimation. In comparison with the FLL in Fig. 1, the proposed TEO-based estimator increases the FLL computational burden by 2 additions and the frequency adaptation block remains unchanged.

The SOGI-TEO cell in Fig. 2, as in the case of SOGI-FLL for the 3 ϕ DSOGI-FLL [11], can be used as building block for the proposed DSOGI-TEO structure in 3 ϕ -3w power converters (Fig. 3). Two SOGI-TEO cells are used, one for each output of the Clarke transform, $T_{\alpha\beta}$. The input for the TEO based frequency estimator is due to the contribution of both cells, i.e. $\frac{\bar{\psi}_\alpha + \bar{\psi}_\beta}{2}$. With the FLL locked, in-phase and in-quadrature components due to the SOGI filters are used to extract the fundamental positive sequence (FPS).

From (8) and the overall methods depicted in Fig. 2 and Fig. 3, the proposal dynamics are dominated by the frequency adaptation algorithm and the selected value for γ_{TEO} .

III. SIMULATION RESULTS

The performances of the proposed DSOGI-TEO, the DSOGI-FLL and the DDSRF-PLL [12] have been evaluated in simulation with MATLAB/Simulink®. For comparison purposes, the same parameters ($k_{SOGI} = \sqrt{2}$, $\gamma_{TEO} = \gamma_{FU} =$

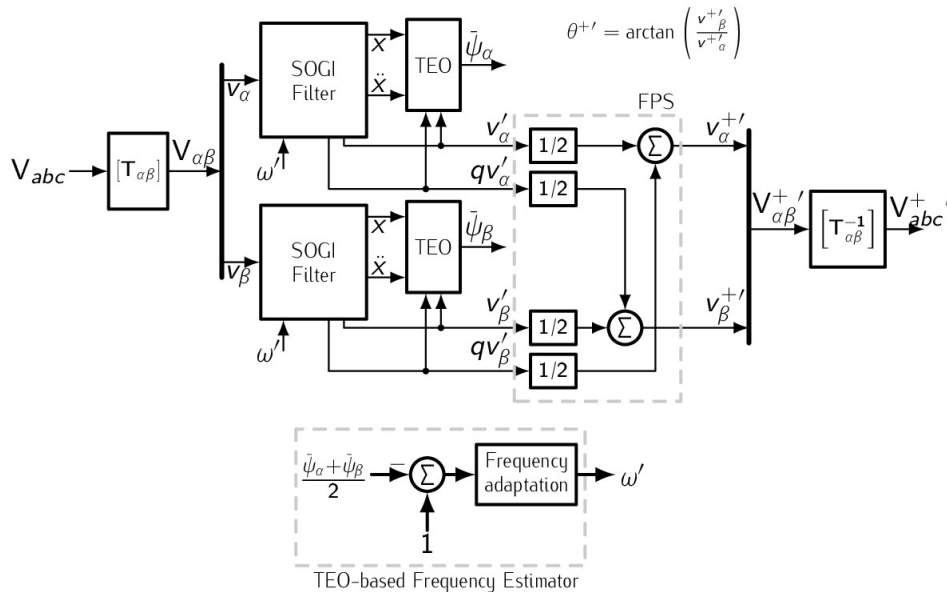


Fig. 3. Proposed 3 ϕ DSOGI-TEO.

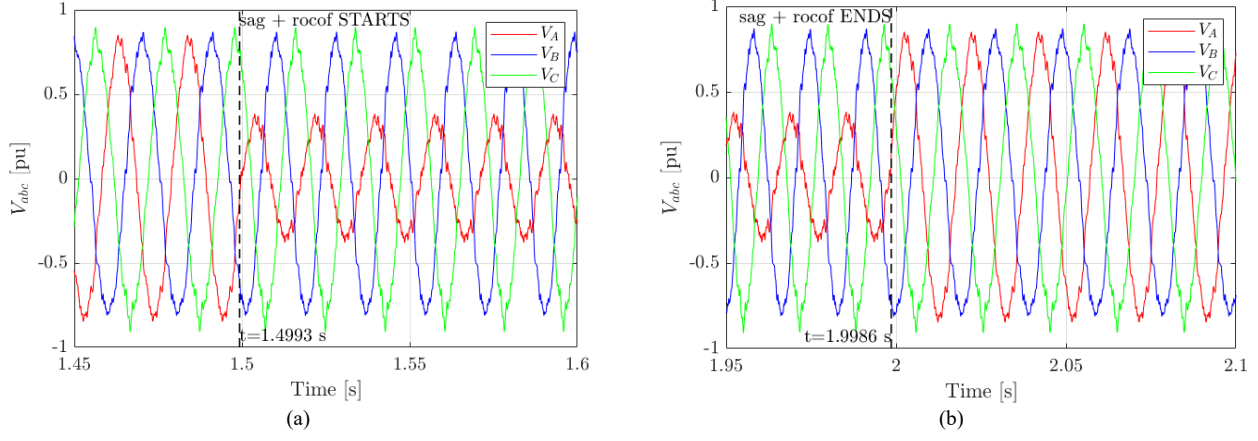


Fig. 4. Type-A 48.05 % voltage sag plus frequency ROCOF +5 Hz/s. Grid voltages. a) sag + ROCOF start and b) sag + ROCOF end. $V_{base} = 400$ V, $\Theta_{base} = 360^\circ$, $f_{base} = 50$ Hz.

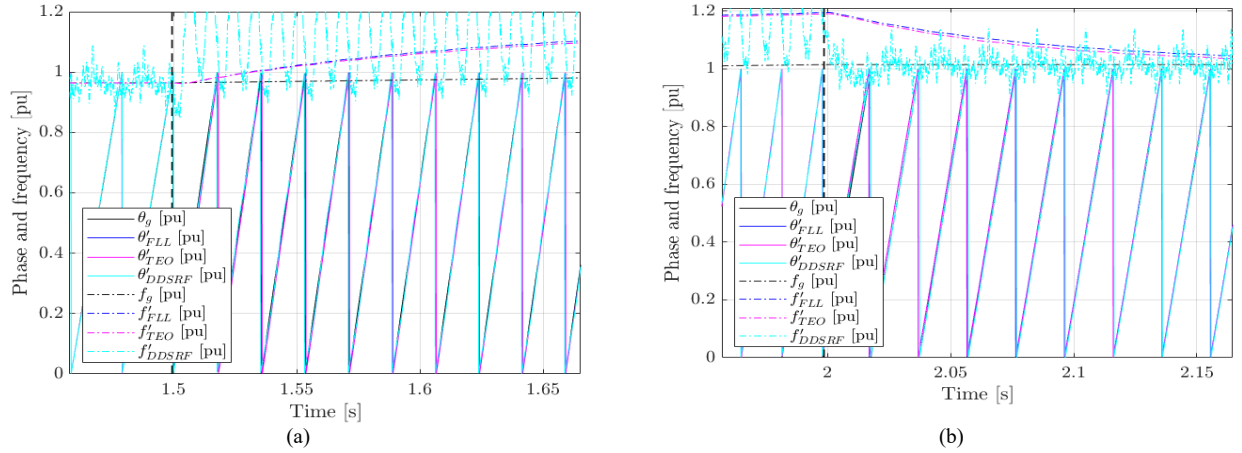


Fig. 5. Type-A 48.05 % voltage sag plus frequency ROCOF +5 Hz/s. Estimated grid frequency and phase a) initial and b) ending transients. $V_{base} = 400$ V, $\Theta_{base} = 360^\circ$, $f_{base} = 50$ Hz.

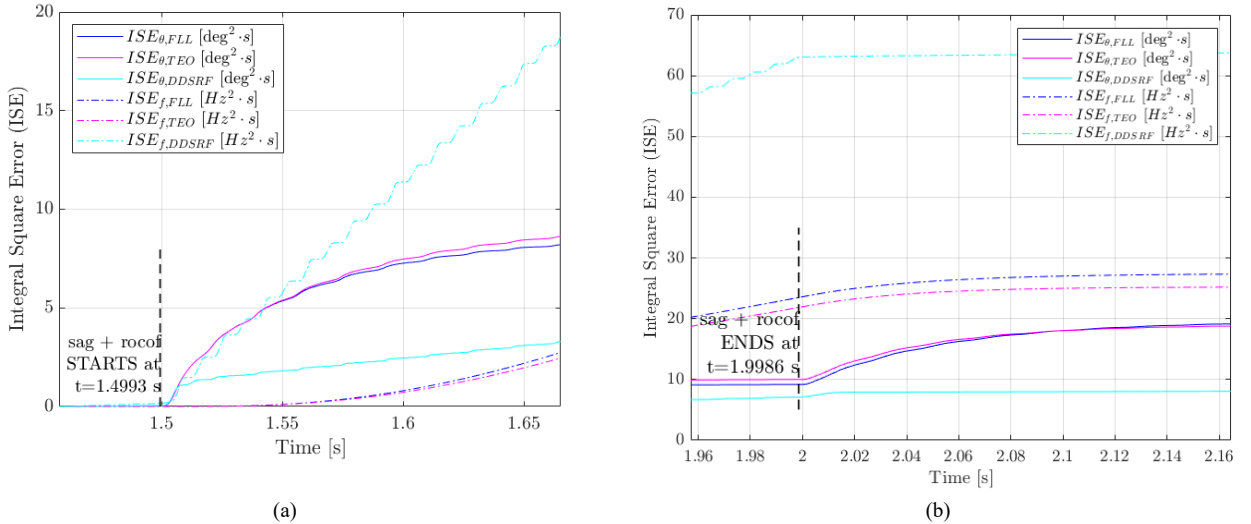


Fig. 6. Type-A 48.05 % voltage sag plus frequency ROCOF +5 Hz/s. Integral Square Error, a) initial and b) ending transients. $V_{base} = 400$ V, $\Theta_{base} = 360^\circ$, $f_{base} = 50$ Hz.

10, $\omega_0 = 2\pi 50$ rad/s) are used in SOGI and SOGI-TEO. However, DDSRF-PLL use the configuration parameters of [12].

Fig. 4 shows the grid voltage waveforms for a 48.05 % @ 518.4 ms voltage sag plus 5 Hz/s rate-of-change-of-frequency (ROCOF). The THD_v and initial grid frequency are 6.8 % and

48.74 Hz, respectively. Moreover, the fundamental is slightly unbalanced, according to the limits in the EN-61000.

Before the initial transient at 1.5184 s, (Fig. 4.a and 4.b) both the DSOGIs perform similarly as shown by angle and frequency estimations plotted in Fig. 5 and the Integral Square Error (ISE) for both estimations (Fig. 6.a) but, after the

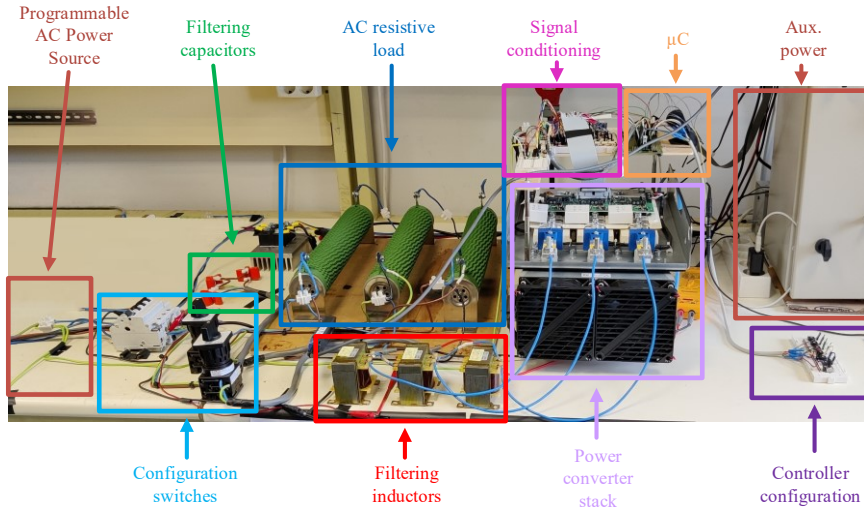


Fig. 7. Laboratory setup.

transient, the DSOGI-TEO reacts faster, stabilizing the phase error in less than 160 ms. From Figs. 5.b and 6.b, before the transient ends, both DSOGIs are tracking the grid angle properly but the estimation ISE still grows due to the ROCOF. After the ending transient, again DSOGI-TEO is faster but results in greater frequency estimation ripple than SOGI. On the contrary, the DDSRF-PLL presents the smallest phase error in all the tests carried out (Fig. 5 and 6). However, its estimated frequency presents a high ripple of up to ± 5 Hz under test conditions, which makes this signal not recommended for applications that use it as a reference signal in control.

IV. EXPERIMENTAL RESULTS

The proposed DSOGI-TEO and both the DSOGI-FLL and DDSRF-PLL have been tested experimentally with the 3 ϕ laboratory setup in Fig. 7. The electrical power grid is emulated with an AMX Series[®] programmable power source from Pacific. The grid-following inverter consists of a power converter stack SKS SL 20 GD/10-E4P1 from Semikron. A LC filter ($L = 1.5$ mH, $C = 3$ μ F) and a signal conditioning circuitry. Also, to ensure that the injected power does not exceed the programmable power source capability, $47 \Omega @ 1.5$ kW resistive loads are connected. The inverter performance is evaluated by means of the precision power analyzer PPA5500 from Newtons4th. The power stack is controlled by means of a TMS320F28335 Control Card, from Texas Instruments, operating at a sampling frequency of 10 kHz. The controller consists of an inner current control loop with decoupled PI controllers in the positive RRF [13]. The reference current per phase is set to 5 A. The estimated grid frequency is scaled, and the digital-to-analog conversion is accomplished by means of a dedicated enhanced PWM module and a first-order low-pass-filter, with a 967.12 Hz cutoff frequency.

Figure 8 shows the responses of DSOGI-FLL (a) and DSOGI-TEO (b) based controllers to +2 Hz frequency steps when a pure sinusoidal grid voltage is used. In comparison with the DSOGI-FLL, the time response due to the proposed DSOGI-TEO is 16 % shorter and similar power factors are achieved by both synchronization methods. Preliminary tests with DDSRF-PLL, in Fig. 8.c, show that this PLL results in a 90 $^\circ$ shifting of the estimated grid phase (channel 6 in Fig. 8.c)

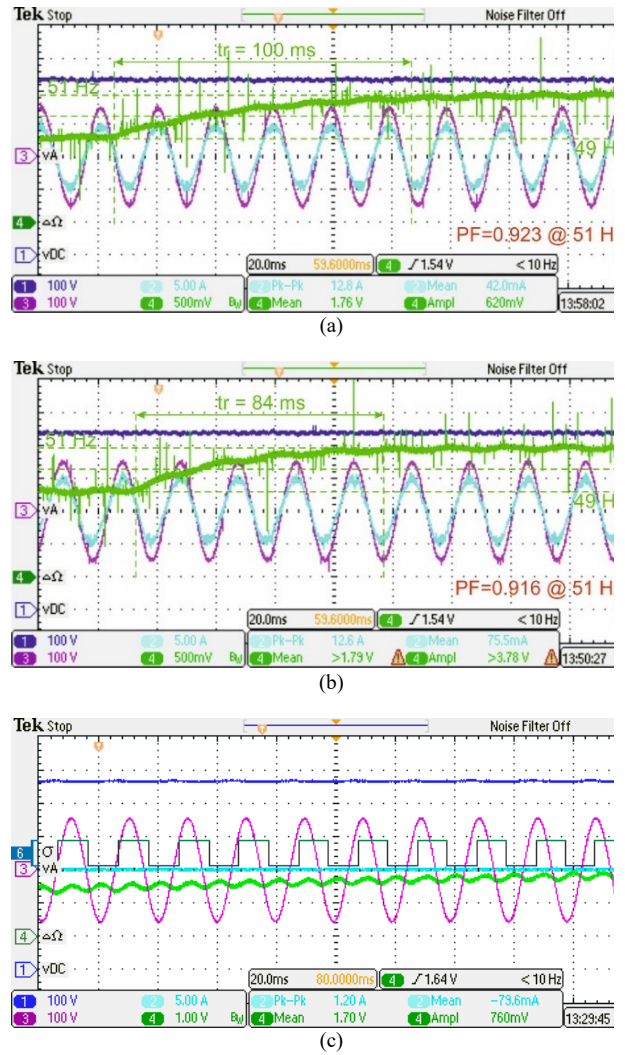


Fig. 8. Frequency step (49 Hz to 51 Hz). a) DSOGI-FLL ($\gamma_{FLL} = 20$), b) DSOGI-TEO and c) DDSRF-PLL ($\gamma_{TEO} = 20$). Blue: DC voltage, magenta [100 V/div]: phase A grid voltage [100 V/div], cyan: phase A line current [5 A/div], green: estimated frequency [1.5 Hz/div]. Time [20 ms/div].

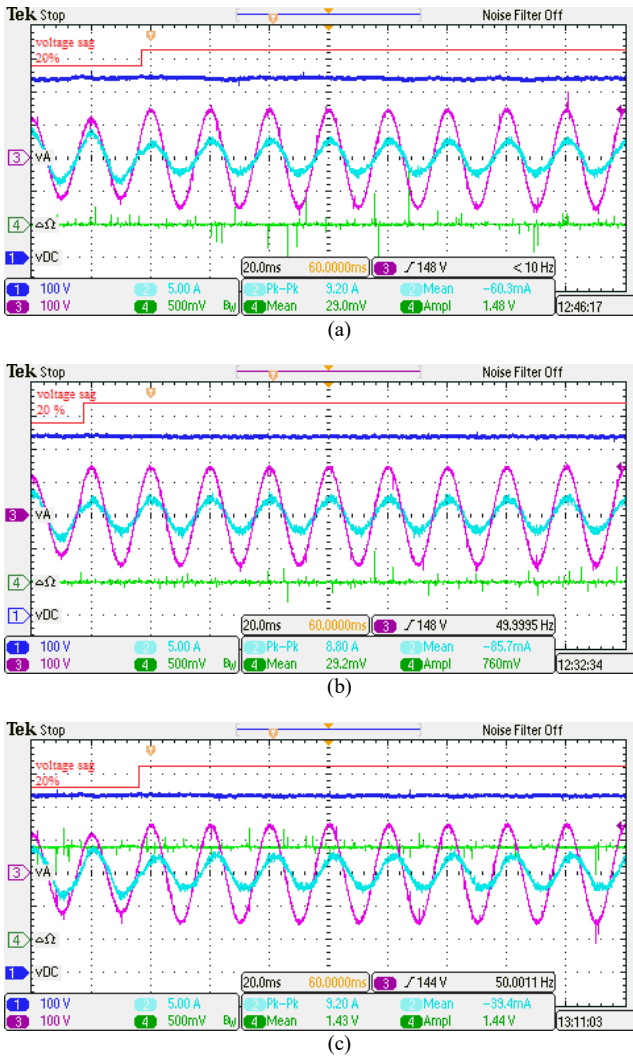


Fig. 9. Voltage sag (20 %). a) DSOGI-FLL ($\gamma_{FLL} = 20$), b) DSOGI-TEO ($\gamma_{TEO} = 20$) and c) DDSRF-PLL. Blue: DC voltage, magenta [100 V/div]: phase A grid voltage [100 V/div], cyan: phase A line current [5 A/div], green: estimated frequency [1.5 Hz/div]. Time [20 ms/div].

and, to prevent damaging the laboratory setup, no further tests with these operation conditions were carried out.

Fig. 9 presents the response of the three strategies analyzed at the ending transient of a 20% voltage dip in phase A, with pure sinusoidal grid voltage at 50 Hz. DSOGI-FLL and DSOGI-TEO present similar behaviors, with response times shorter than two cycles at the fundamental frequency. The DDSRF-PLL presents the worst behavior, having a response time larger than 160 ms and injecting a significant amount of reactive power during the transient.

V. CONCLUSIONS

A novel frequency estimator based on the Teager Energy Operator (TEO) is proposed to be used in combination with SOGI filter cells. The proposed method only uses inner SOGI cell variables. The simulation and experimental results obtained show that the proposed method, i.e. DSOGI-TEO, under the same operation conditions than the DSOGI-FLL and the DDSRF-PLL, achieves a similar performance in

steady-state. However, the transient response due to DSOGI-TEO results in a faster tracking of the fundamental positive sequence (FPS) with a greater frequency estimation overshoot and ripple than DSOGI-FLL.

REFERENCES

- [1] P. Rodriguez, A. Luna, M. Ciobotaru, R. Teodorescu, and F. Blaabjerg, "Advanced Grid Synchronization System for Power Converters under Unbalanced and Distorted Operating Conditions," in *IECON 2006 - 32nd Annual Conference on IEEE Industrial Electronics*, Paris, Nov. 2006, pp. 5173–5178. doi: 10.1109/IECON.2006.347807.
- [2] P. Rodriguez, A. Luna, I. Candela, R. Mujal, R. Teodorescu, and F. Blaabjerg, "Multiresonant Frequency-Locked Loop for Grid Synchronization of Power Converters Under Distorted Grid Conditions," *IEEE Trans. Ind. Electron.*, vol. 58, no. 1, pp. 127–138, Jan. 2011, doi: 10.1109/TIE.2010.2042420.
- [3] S. Golestan, J. M. Guerrero, Juan. C. Vasquez, A. M. Abusorrah, and Y. Al-Turki, "Modeling, Tuning, and Performance Comparison of Second-Order-Generalized-Integrator-Based FLLs," *IEEE Trans. Power Electron.*, vol. 33, no. 12, pp. 10229–10239, Dec. 2018, doi: 10.1109/TPEL.2018.2808246.
- [4] S. Golestan, J. M. Guerrero, Juan. C. Vasquez, A. M. Abusorrah, and Y. Al-Turki, "Standard SOGI-FLL and Its Close Variants: Precise Modeling in LTP Framework and Determining Stability Region/Robustness Metrics," *IEEE Trans. Power Electron.*, vol. 36, no. 1, pp. 409–422, Jan. 2021, doi: 10.1109/TPEL.2020.2997603.
- [5] C. Zhang, S. Foyen, J. A. Suul, and M. Molinas, "Modeling and Analysis of SOGI-PLL/FLL-Based Synchronization Units: Stability Impacts of Different Frequency-Feedback Paths," *IEEE Trans. Energy Convers.*, vol. 36, no. 3, pp. 2047–2058, Sep. 2021, doi: 10.1109/TEC.2020.3041797.
- [6] S. Golestan, J. M. Guerrero, A. M. Abusorrah, J. C. Vasquez, and Y. Al-Turki, "LTP Modeling and Stability Assessment of Multiple Second-Order Generalized Integrator-Based Signal Processing/Synchronization Algorithms and Their Close Variants," *IEEE Trans. Power Electron.*, vol. 37, no. 5, pp. 5062–5077, May 2022, doi: 10.1109/TPEL.2021.3125743.
- [7] J. Matas, H. Martin, J. de la Hoz, A. Abusorrah, Y. A. Al-Turki, and M. Al-Hindawi, "A Family of Gradient Descent Grid Frequency Estimators for the SOGI Filter," *IEEE Trans. Power Electron.*, vol. 33, no. 7, pp. 5796–5810, Jul. 2018, doi: 10.1109/TPEL.2017.2748920.
- [8] S. Golestan, J. M. Guerrero, F. Musavi, and J. C. Vasquez, "Single-Phase Frequency-Locked Loops: A Comprehensive Review," *IEEE Trans. Power Electron.*, vol. 34, no. 12, pp. 11791–11812, Dec. 2019, doi: 10.1109/TPEL.2019.2910247.
- [9] X. He, H. Geng, and G. Yang, "A Generalized Design Framework of Notch Filter Based Frequency-Locked Loop for Three-Phase Grid Voltage," *IEEE Trans. Ind. Electron.*, vol. 65, no. 9, pp. 7072–7084, Sep. 2018, doi: 10.1109/TIE.2017.2784413.
- [10] A. Gałężia and A. Orłowska-Gałężia, "Application of Teager-Kaiser's Instantaneous Frequency for Detection of Delamination in FRP Composite Materials," *Materials*, vol. 14, no. 5, p. 1154, Mar. 2021, doi: 10.3390/ma14051154.
- [11] P. Rodríguez, A. Luna, R. S. Muñoz-Aguilar, I. Etxeberria-Otadui, R. Teodorescu, and F. Blaabjerg, "A Stationary Reference Frame Grid Synchronization System for Three-Phase Grid-Connected Power Converters Under Adverse Grid Conditions," *IEEE Trans. Power Electron.*, vol. 27, no. 1, pp. 99–112, Jan. 2012, doi: 10.1109/TPEL.2011.2159242.
- [12] P. Rodriguez, J. Pou, J. Bergas, J. I. Candela, R. P. Burgos, and D. Boroyevich, "Decoupled Double Synchronous Reference Frame PLL for Power Converters Control," *IEEE Trans. Power Electron.*, vol. 22, no. 2, pp. 584–592, Mar. 2007, doi: 10.1109/TPEL.2006.890000.
- [13] F. D. Freijedo *et al.*, "Tuning of Synchronous-Frame PI Current Controllers in Grid-Connected Converters Operating at a Low Sampling Rate by MIMO Root Locus," *IEEE Trans. Ind. Electron.*, vol. 62, no. 8, pp. 5006–5017, Aug. 2015, doi: 10.1109/TIE.2015.2402114.